The electronic structure of the ground and excited states of Mg_2^+ and Mg_2[a)]

W. J. Stevens

Time and Frequency Division, National Bureau of Standards, Boulder, Colorado 80302

M. Krauss

Physical Chemistry Division, National Bureau of Standards, Washington, D.C. 20234
(Received 13 January 1977)

The ground and excited valence states of Mg_2^+ and Mg_2 are calculated using the multiconfiguration self-consistent-field method. The energy curves of the $X\,^1\Sigma_g^+$, $^3\Pi_g$, $^3\Sigma_u^+$, $^3\Pi_u$, $^3\Sigma_g^+$, $^1\Pi_g$, $^1\Sigma_u^+$, $^1\Pi_u$, and $2\,^1\Sigma_g^+$ μ states of Mg_2 and the $^2\Sigma_u^+$ and $^2\Pi_\mu$ curves of Mg_2^+ are obtained for internuclear separations between 4 and 15 bohr. All of the excited states except the $^3\Pi_u$ and $^3\Sigma_g^+$ are found to be bound while the ground state is a weakly bound van der Waals molecule. Comparison between the calculated and experimentally known $X\,^1\Sigma_g^+$ and $^1\Sigma_u^+$ energy curves shows good agreement for the equilibrium internuclear separation but the calculated D_e (620 cm^{-1}) for the best approximation of the $X\,^1\Sigma_g^+$ state exceeds the experimental value by about 40%, and the calculated D_e for the $^1\Sigma_u^+$ state is smaller than the experimental value of 9387 cm^{-1} by about 1800 cm^{-1}. Analysis of the electronic structure of the excimers shows that the triplet states and the $^1\Pi_g$ state are qualitatively described by covalent molecular orbital theory but all of the other bound singlets require more complicated descriptions including covalent configurational mixing, charge transfer, and Rydberg–covalent configuration mixing. Only the $^1\Pi_u$ state can be unambiguously characterized as a charge transfer state. The Mg_2 states were calculated to provide a model of the Group II excimer systems, which are candidates for the active media of lasers.

I. INTRODUCTION

The Group II metal dimers belong to the broad class of molecules known as excimer systems. They have strongly bound excited states and weakly bound or repulsive ground states. This causes spectral transitions between the excited states and the ground states to appear as broad continua that are shifted far to the red of the corresponding atomic lines. Transitions of this type are ideally suited for laser applications. The repulsive (unbound) nature of the ground state implies easily achieved inversions. The large widths of the continuum bands imply tunability, and a relatively small radiative cross section which permits considerable energy storage.

Until recently very little information was available about the nature of the excited states of the Group II dimers. Although broad band emission continua have been observed for several species,[1] only in the case of Mg_2[2,3] have structured spectra been observed and analyzed to yield information about the dimer potential energy curves. Extensive configuration interaction calculations on the electronic states of Be_2 were published by Bender and Davidson.[4] However, Be_2 is not a valid prototype divalent metal system due to the absence of p or d electrons in the core. In addition, the $^3P+{}^3P$ energy asymptote is below the $^1S+{}^1P$ for Be + Be, which is different from all other Group IIA and IIB metals. Bender and Davidson found all of the excited states of Be_2 to be bound, which is certainly not typical of the metal systems that have been studied more recently. Calculations on the ground and excited states of Zn_2 have been completed recently by Hay, Dunning, and Raffenetti.[5] Their results are very similar to our results for Mg_2, with a few exceptions which will be mentioned in the discussions to follow.

We have chosen Mg_2 as a prototype Group II metal dimer system because the number of electrons (24) is sufficiently few to allow reasonably accurate *ab initio* calculations. In addition, the $^1\Sigma_g^+$ ground state and $^1\Sigma_u^+$ excited state potentials are known from an analysis of experimental absorption spectra.[2,3,6] The lack of d electrons in the magnesium atomic core is of some concern, but an analysis of other systems such as Zn_2[5] shows the d electrons to be unimportant in the energetics of the low-lying excited states. Extrapolations from Mg_2 to other similar systems is most seriously impeded by the effects of spin–orbit coupling, differences in the sizes (radial extents) of the valence electronic distributions, and the differences in ionization potentials between the Group IIA and IIB metals.

We have calculated potential energy curves for all of the states of Mg_2 arising from the $^1S+{}^1S$, $^1S+{}^3P$, and $^1S+{}^1P$ atomic asymptotes, and the lowest $^2\Sigma_u^+$ and $^2\Pi_u$ states of Mg_2^+. We have used multiconfiguration self-consistent-field techniques (MCSCF) to variationally construct approximate solutions to the electronic Schrödinger equation within the space of a large basis set of Slater-type functions (STF). For all states we have attempted to achieve an accuracy of 0.2 to 0.3 eV in the shapes of the potential energy curves in order to insure that the ordering of the states, their relative binding energies, and their relative potential minima are reliable. These results should aid in the interpretation of experimental spectroscopic and kinetic data for systems which are more interesting laser candidates such as Hg_2.

[a)]Supported in part by the Laser Fusion Division, ERDA.

TABLE I. STF[a] basis set for Mg_2.[b]

σ Functions				π Functions			
N	L	M	Zeta	N	L	M	Zeta
1	0	0	14.161	2	1	1	8.527
2	0	0	12.228	2	1	1	4.705
3	0	0	7.091	2	1	1	2.719
2	0	0	3.499	3	1	1	1.168
3	0	0	1.458	3	1	1	0.560
3	0	0	0.891	3	2	1	2.000
2	1	0	8.527	3	2	1	1.000 (0.600)
2	1	0	4.705				
2	1	0	2.719				
3	1	0	1.168				
3	1	0	0.560				
3	2	0	2.000				
3	2	0	1.000 (0.600)				
4	0	0	1.000 (0.600)				

[a]Slater-type functions have the form $X_{NLM} = A_N r^{N-1} e^{-\zeta r} \times Y_{LM}(\theta, \phi)$, where A_N is the normalization and Y_{LM} are the usual spherical harmonics.

[b]An identical basis was placed at each Mg nuclear center.

II. COMPUTATIONAL DETAILS

The calculations described here were carried out with the BISON-MC multiconfiguration self-consistent-field computing system of Das and Wahl.[7] In the MCSCF method the electronic wavefunction is approximated by a superposition of configurations

$$\Psi(1, 2, \cdots, n) = \sum_K A_K \Phi_K \ . \tag{II-1}$$

The configurations are constructed from properly projected Slater determinants over a set of molecular spin orbitals

$$\Phi(1, 2, \ldots, n) = O_{\Lambda, S} \left| \phi_1(1)\, \phi_2(2) \cdots \phi_n(n) \right| , \tag{II-2}$$

where $O_{\Lambda, S}$ represents projection to an eigenfunction of spin and the projection of the angular momentum on the molecular axis. The space parts of the molecular orbitals ϕ are expanded in a basis of Slater-type functions (STF)

$$\phi_i = \sum_j C_{ij} \chi_j \ . \tag{II-3}$$

In the MCSCF procedure the molecular orbital expansion coefficients C_{ij} and the configuration mixing coefficients A_K are determined variationally by minimizing the energy in the electronic Schrödinger equation within the Born–Oppenheimer approximation.

The STF basis for Mg used in these calculations was obtained by augmenting the "nominal" basis for the ^1S state given by Bagus *et al.*[8] Two $3p$ STF's were added to the basis and optimized by minimizing the single configuration self-consistent-field (SCF) energy of the center of spin of the $^{1,3}P$ manifold. Two $3d$ STF's were a added to account for the effect on the molecular wavefunctions of the low-lying Mg $4s$ Rydberg level. The final STF basis is shown in Table I. Two exponents are shown for the diffuse $3d$ and $4s$ STF's because the $^1\Sigma_u^+$, $2\,^1\Sigma_g^+$, $^1\Pi_u$, $^1\Pi_g$, and $^3\Sigma_g^+$ calculations were carried out with the smaller exponent (0.6). The energetic dependence on these exponents was small. Our experience has been that a basis set of this quality for the neutral system is also adequate for the positive ion (in this case case Mg_2^+).

III. Mg_2^+, $^2\Sigma_u^+$ and $^2\Pi_u$ ION STATES

The metal atoms, such as magnesium, have ionization potentials which are rather small [I. P. (Mg) = 7.64 eV], and the atomic Rydberg levels are energetically not very far above the highest lying valence states. In magnesium the $4s$, ^3S and $4s$, ^1S Rydberg levels lie just 0.762 and 1.048 eV above the $3p$, ^1P excited valence state, respectively. If the ionization potential of the dimer molecule is much lower than that of the atom, and if the molecular quantum defect is not too much different from the atomic quantum defect, then it is possible that the molecular Rydberg levels are very low lying and may affect the high-lying molecular valence states through valence–Rydberg mixing. For this reason we decided to study the lowest bound Mg_2^+ states in order to find the difference between the atomic and molecular ionization potentials as compared to the valence–Rydberg splitting in the atom.

The ground state ($^1\Sigma_g^+$) configuration of Mg_2 can be written as

$$4\sigma_g^2\, 4\sigma_u^2\, (^1\Sigma_g^+), \tag{III-1}$$

where we have neglected the core orbitals and $4\sigma_{g,u} \rightarrow (1/\sqrt{2})(3s_A \pm 3s_B)$ asymptotically. Two one-electron ionizations are possible, giving the states

$$\begin{aligned} &4\sigma_g^2\, 4\sigma_u\, (^2\Sigma_u^+), \\ &4\sigma_g\, 4\sigma_u^2\, (^2\Sigma_g^+). \end{aligned} \tag{III-2}$$

The $^2\Sigma_u^+$ state is predicted to be bound and is the lowest-lying state of Mg_2^+ dissociating to $Mg(^1S) + Mg^+(^2S)$. The single configuration $4\sigma_g^2\, 4\sigma_u$ is sufficient to give a formally correct description of the molecular ion as well as the asymptotic dissociation limit. However, within the single configuration approximation the dissociated atom and atomic ion are restricted to have the same electronic core distributions. This will cause the asymptotic energy to be artifically high relative to the minimum molecular energy, thereby overestimating the dissociation energy. However, the effect is rather small compared to the single configuration approximation and the calculated asymptotic energy is only 0.18 eV above the sum of the Hartree–Fock atom and ion energies.[9] Unfortunately, the Hartree–Fock atomic ionization potential is about 1 eV lower than the experimental value, which causes the Rydberg levels to be too low in energy and exaggerates the Rydberg–valence mixing unless the differential correlation energy between the atom and ion is taken into account.

The first excited Mg_2^+ asymptote is $Mg(^3P) + Mg^+(^2S)$, which lies 2.7 eV above the ground state asymptote. Ordinarily, we would not be concerned with ion states that dissociate to higher-lying asymptotes, but in this case it appeared that a deeply bound molecular ion state might arise from $^3P + {}^2S$. The state is a $^2\Pi_u$ state, which

TABLE II. Potential energy curves for bound Mg_2^+ ions.

R (bohr)	$^2\Sigma_u^+$ (cm^{-1}) [a]	$^2\Pi_u$ (cm^{-1}) [b]
4.0	...	−4442
4.5	−1231	...
5.0	−6324	−12971
5.5	−8221	−12051
6.0	−8430	−10036
6.5	−7819	...
7.0	−6871	−5852
7.5	−5842	...
8.0	...	−3207
9.0	−3223	...
12.0	−810	...
15.0	...	−23

[a]Asymptotic energy = −398.97945 hartree.
[b]Asymptotic energy = −398.889731 hartree. 1 hartree = 219474.6 cm^{-1}.

is asymptotically described by the linear combination of two configurations

$$\frac{1}{\sqrt{2}}\,4\sigma_g^2\,1\pi_u - \frac{1}{\sqrt{2}}\,4\sigma_u^2\,1\pi_u\,. \qquad \text{(III-3)}$$

At smaller nuclear separations the first configuration will dominate and should produce considerable binding.

The calculated results for our single configuration $^2\Sigma_u^+$ state and double configuration $^2\Pi_u$ state are tabulated in Table II and displayed in Fig. 1. In the plot we have adjusted the molecular asymptotes to agree with the known atomic splittings. The binding energy of the $^2\Sigma_u^+$ state is about 1.1 eV. Since the ground state is repulsive, this causes the ionization potential of Mg_2 to be at least 1.1 eV less than the ionization potential of the atom. For that reason we believe the molecular Rydberg states are much lower lying than the atomic Rydberg levels. Consequently, they could play an important role in the high-lying molecular valence states.

Although the $^2\Pi_u$ ion state arising from the $^3P + {}^2S$ asymptote was found to be more bound (1.36 eV) than $^2\Sigma_u^+$, the binding is not sufficient to make that state a serious contender for the lowest molecular ion state.

These ion calculations also yield some information about the long-range overlap effects in these metallic systems. Since the dipole polarizability of the ^1S Mg atom is known,[10] it is easy to see that the binding energy at 12 bohr in the $^2\Sigma_u^+$ state exceeds the ion-induced dipole attraction by a factor of 2. This indicates that overlap and charge exchange effects are significant even for distances as large as 12 bohr. For the $^2\Pi_u$ state no comparison is possible since neither the quadrupole moment nor the dipole polarizability of the ^3P excited state is known. For favorable orientations of the $3p$ atomic orbital the overlap effects are likely to be larger than in the ground state.

IV. THE $X^1\Sigma_g^+$ GROUND STATE OF Mg_2

A. Hartree–Fock results

The ground state of Mg_2 arises from two ^1S atoms and is principally represented by the single configuration

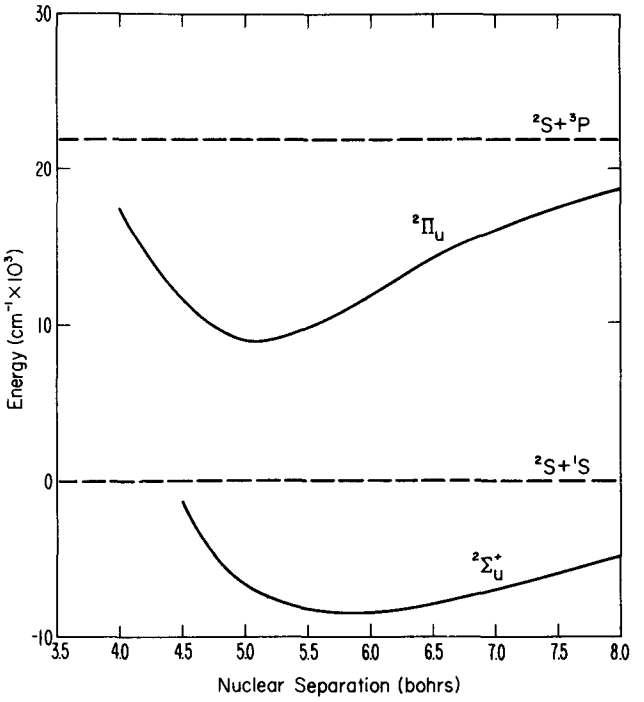

FIG. 1. Bound states of the Mg_2^+ ion (1 bohr = 0.5291772 $\times 10^{-8}$ cm).

[core] $4\sigma_g^2\,4\sigma_u^2$, where [core] is taken to represent the electronic configuration of the inner shell electrons. Asymptotically ($R \to \infty$), the valence molecular orbitals have the form

$$4\sigma_g \to \frac{1}{\sqrt{2}}(3s_A + 3s_B)\,,$$
$$4\sigma_u \to \frac{1}{\sqrt{2}}(3s_A - 3s_B)\,, \qquad \text{(IV-1)}$$

where A and B are used to label the nuclear centers. The single configuration wavefunction is usually referred to as the Hartree–Fock wavefunction.

As is the case with all closed-shell atomic interactions, the Hartree–Fock approximation produces a totally repulsive potential energy curve when a sufficiently saturated basis set is used. Our Hartree–Fock results are tabulated in Table III, and plotted in Fig. 2.

TABLE III. Potential energy curves for the $X^1\Sigma_g^+$ state of Mg_2.[a]

R (bohr) [b]	Hartree–Fock [c]	Hartree–Fock + van der Waals correlation [c]	Hartree–Fock + intra-atomic correlation [d]
4.50	13905.7	...	...
5.00	7582.8	4394.1	9952.1
5.50	4196.6	1427.5	6143.8
6.00	2388.1	55.3	3878.4
6.50	1404.6	−462.7	2486.0
7.00	850.5	−610.1	1602.6
7.50	524.5	−601.8	1030.3
12.00	1.1	−96.1	15.4

[a]Energies in cm^{-1}.
[b]1 bohr = 0.5291772 Å.
[c]Asymptotic energy = −399.22868 hartree.
[d]Asymptotic energy = −399.28710 hartree. 1 hartree = 219474.6 cm^{-1}.

To our knowledge there are no other published Hartree–Fock calculations on Mg_2 with which we can compare our results. However, very recently results have been presented by Scheingraber and Vidal[3,6] in which the repulsive part of the $X\,^1\Sigma_g^+$ molecular potential has been determined from laser-induced fluorescence measurements. In their experiment a single vibrational level of the $^1\Sigma_u^+$ state is selectively excited from the ground state van der Waals well with a laser. The radiative transition from the excited vibrational level back to the ground state yields bound–free as well as bound–bound radiation. The bound–free transition results in an oscillatory continuum which is characteristic of transitions from a high-lying vibrational level of a bound state to the continuous levels of an unbound state.[11] Scheingraber and Vidal fit the oscillations in the observed spectrum by adjusting the parameters of a model ground state repulsive potential while calculating quantum mechanical bound–free Frank–Condon factors for the known excited state vibrational–rotational level which was selectively excited. These fits did not take into account the variation of the dipole transition moment with internuclear distance. They assumed an exponential model for the repulsive wall of the ground state potential with the form $V(r) = \exp\{\sum_n c_n[(r - r_e)/r_e]^n\}$. The constants obtained from their fit to the continuum (due to excited state $v' = 7$, $J' = 61$) are $c_0 = 0.700$, $c_1 = 52.08$, $c_2 = -145.70$, $c_3 = 180.71$, and $r_e = 3.8894$, with energies in cm^{-1} and distances in Å (and a range of validity from 2.68 to 3.28 Å). Their fitted curve is plotted in Fig. 2. Our calculated Hartree–Fock potential differs markedly from the experimentally derived potential, which indicates that electron correlation effects must be very important in determining the true ground state potential for Mg_2.

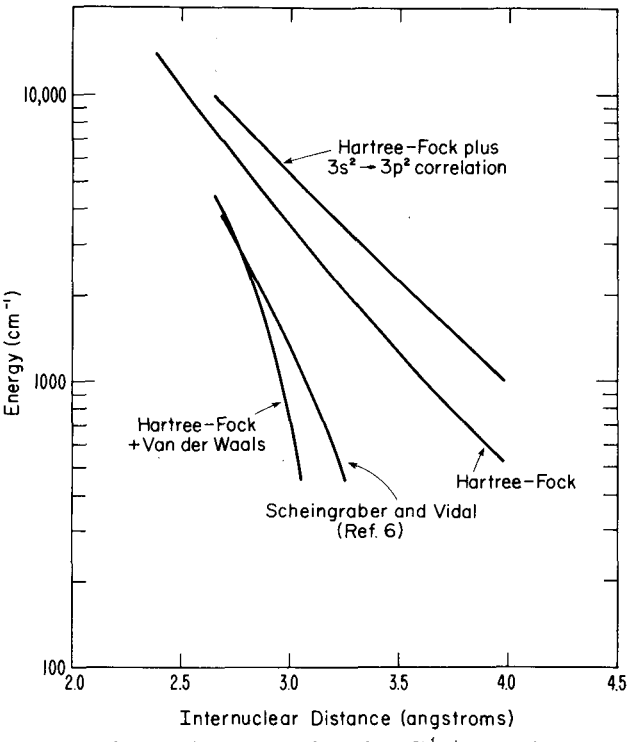

FIG. 2. The repulsive part of the Mg_2 $X\,^1\Sigma_g^+$ ground state potential.

B. Calculation of the van der Waals terms

Mg_2 is the only molecular system for which an accurate RKR potential for the van der Waals well has been obtained from spectroscopic data.[2] The long range inverse power series expansion of the potential has been studied in detail by Stwalley.[12]

In 1970, Wahl and co-workers[13] introduced an *ab initio* technique for adding configurations to the Hartree–Fock wavefunction which account for the van der Waals atom–atom interactions at large values of R. First, the Hartree–Fock wavefunction is written in localized (valence-bond) form. For Mg_2 we have

$$[\text{core}]4\sigma_g^2\,4\sigma_u^2 \rightarrow [\text{core}]_A[\text{core}]_B\,3s_A^2\,3s_B^2\ . \qquad \text{(IV-2)}$$

Next, with the Hartree–Fock orbitals frozen, double excitations are added which are composed of a single excitation on each atom such as

$$\Psi = 3s_A^2\,3s_B^2 + 3s_A\,\phi_A\,3s_B\phi_B\ , \qquad \text{(IV-3)}$$

where we have dropped the core notation and ϕ represents an MCSCF optimized orbital which turns out to be localized because of the localized nature of the principal (Hartree–Fock) orbitals. It is not hard to show that configurations of this type give rise to dispersion interactions at large R (zero-overlap region) and disappear as $R \rightarrow \infty$. There are two possible deficiencies in this approach to the van der Waals interactions. First, as the atoms begin to overlap, orthogonality makes the complete localization of the Hartree–Fock orbitals impossible. Thus, it becomes increasingly hard to distinguish interatomic and intra-atomic correlation effects as the overlap increases. All van der Waals wells have their minima in the intermediate region where the atom–atom overlap is small, but not negligible. Secondly, if intra-atomic correlation terms are added to the wavefunction, their contribution can change as a function of R[14] and they can also interact with the interatomic van der Waals terms.[15] Despite these shortcomings, Bertoncini and Wahl[13,14] have obtained remarkable results for the He_2 van der Waals interaction using the MCSCF procedure outlined above. Similar calculations have also been carried out on HeH and LiHe,[16] ArH,[17] and Ne_2,[18] all with good results.

Since the outer shell of Mg is $3s^2$, the van der Waals terms to be added to the Hartree–Fock configuration are similar to those used in the He_2 calculation.[13,14] The configurations are shown in Table IV. Configurations 2 and 3 are the dispersion configurations. Configurations 4–8 do not represent long-range $1/R$-type dispersion interactions, but they are important at intermediate distances, where overlap effects start to occur. At large R, where the interatomic overlap is zero, configurations 4–8 do not contribute to the wavefunction. We found it necessary to add configuration 8 in order to have an energy lowering from the Hartree–Fock energy which was close to the sum of the energy lowerings for configurations 2 and 3 and 4–7 taken separately.

The potential energy curve obtained with the eight con-

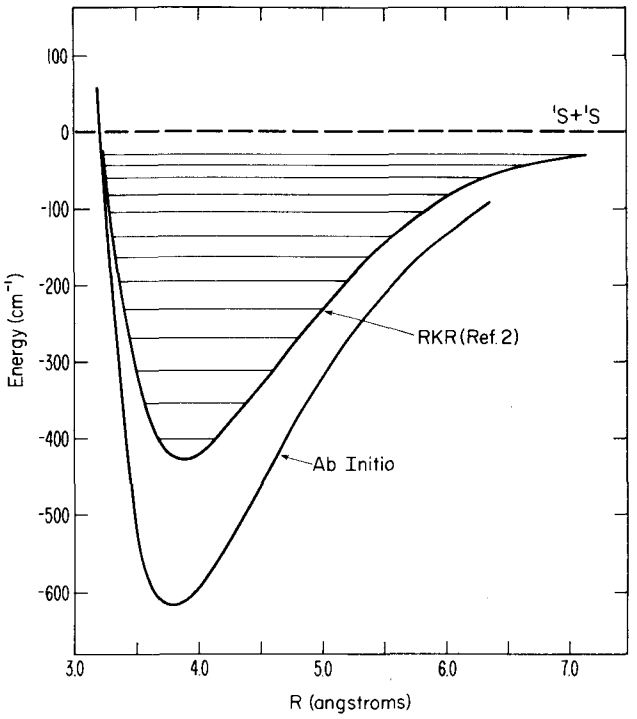

FIG. 3. Comparison of theoretical and experimental (RKR) van der Waals wells for the $X\,^1\Sigma_g^+$ state of Mg_2.

figuration wavefunction is tabulated in Table III and plotted in Figs. 2 and 3 along with the experimental potential curve of Balfour and Douglas.[2] The *ab initio* curve predicts a D_e which is too large by about 40%. The theoretical R_e is 3.8 Å as compared to the experimental value of 3.89 Å. There are several possible explanations for the large D_e value. Since the magnesium atom basis set is only a "nominal" one,[8] the expansion error in the atomic Hartree–Fock energy for Mg (^1S) is 0.001 hartree (219 cm^{-1}) relative to the exact nonrelativistic numerical Hartree–Fock energy.[19] It is possible that the expansion error in the molecular Hartree–Fock energy in the overlap region is less than 438 cm^{-1} (twice the atomic error) due to the superposition of the two atomic basis sets. This would cause an artificial deepening of the potential energy curve. It is also possible that the intra-atomic correlation of the magnesium atoms changes strongly with overlap. To test this we added $3s^2 \rightarrow 3p^2$ intra-atomic excitations to the localized molecular Hartree–Fock wavefunction as shown in Table V. The total asymptotic energy lowering due to these configurations is 0.05842 hartree (two atoms), while near the van der Waals R_e the lowering is 0.05501 hartree. The potential energy curve obtained with the five configuration wavefunction is tabulated in Table III and plotted in Fig. 2. The atomic correlation changes significantly with R, and substantially modifies the repulsive energy curve as shown in Fig. 2. The effect is so great that if the changes in energy from the Hartree–Fock at each value of R due to intra-atomic correlation were added to the van der Waals potential, the van der Waals well would almost disappear. Also, in Fig. 2 reasonable agreement is seen between the repulsive part of the "Hartree–Fock plus van der Waals" (HFVDW) potential and the experimentally derived potential of Scheingraber and Vidal.[3,6] If the atomic correlation changes were added to the HFVDW potential, the agreement would be lost. Quite obviously there is strong coupling between the interatomic and intra-atomic configurations. Due to computer limitations we were not able to combine the two effects in one calculation. We would suggest, however, that the ground state of Mg_2 is a good test case for any theory of interatomic forces at intermediate distances.

TABLE IV. van der Waals configurations for the $X\,^1\Sigma_g^+$ state of Mg_2.

Configuration no.	Occupancies							No. of couplings
	$3s_A$	$3s_B$	$\phi_{\sigma A}$	$\phi_{\sigma B}$	$\phi_{\pi A}$	$\phi_{\pi B}$	ϕ'_{π}	
1	2	2	0	0	0	0	0	[1]
2	1	1	1	1	0	0	0	[2]
3	1	1	0	0	1	1	0	[2]
4	1	1	2	0	0	0	0	[1]
5	1	1	0	2	0	0	0	[1]
6	1	1	0	0	2	0	0	[1]
7	1	1	0	0	0	2	0	[1]
8	1	1	0	0	0	0	2	[1]

TABLE V. Intra-atomic correlation configurations for the $X\,^1\Sigma_g^+$ state of Mg_2.

Configuration no.	Occupancies						No. of couplings
	$3s_A$	$3s_B$	$\phi_{\sigma A}$	$\phi_{\sigma B}$	$\phi_{\pi A}$	$\phi_{\pi B}$	
1	2	2	0	0	0	0	[1]
2	0	2	2	0	0	0	[1]
3	2	0	0	2	0	0	[1]
4	0	2	0	0	2	0	[1]
5	2	0	0	0	0	2	[1]

V. THE EXCITED STATES OF Mg_2

A. Analysis of electronic structure

The excited states of Mg_2 being considered in this study are those arising from the $^1S + {}^3P$ and $^1S + {}^1P$ atomic asymptotes. However, the role of configuration mixing involving states arising from higher-lying asymptotes is important to the understanding of the electronic structure of the low-lying excited molecular states. The various atomic asymptotes and molecular states we will be referring to in this discussion are shown in Table VI.

In addition to the asymptotic behavior, the character of the molecular orbitals near the equilibrium geometry of the excited states will be examined. Usually, this resolves into an analysis of the bonding character of the valence molecular orbitals listed in Table VII. From overlap considerations it is obvious that the $4\sigma_g$, $5\sigma_g$, and $2\pi_u$ orbitals are bonding while the others are not. The usual aufbau of dominant single configurations for the bound excited states would add the available valence orbitals to the bound ion core $4\sigma_g^2\,4\sigma_u$. Four states are then predicted to be stable, the $4\sigma_g^2\,4\sigma_u\,2\pi_u$ ($^3\Pi_g$ and $^1\Pi_g$) and $4\sigma_g^2\,4\sigma_u\,5\sigma_g$ ($^3\Sigma_u^+$ and $^1\Sigma_u^+$). However, the calculations show that there are two other slightly bound states.

TABLE VI. Asymptotic states of Mg_2.

A	B	$E(cm^{-1})$	Molecular states
^1S	^1S	0	$^1\Sigma_g^+$
^1S	$^3P_0$	21 850	$^3\Sigma_g^+$, $^3\Sigma_u^+$, $^3\Pi_g$, $^3\Pi_u$
^1S	^1P	35 051	$^1\Sigma_g^+$, $^1\Sigma_u^+$, $^1\Pi_g$, $^1\Pi_u$
^1S	^3S	41 197	$^3\Sigma_g^+$, $^3\Sigma_u^+$
^1S	$2\,^1S$	43 503	$^1\Sigma_g^+$, $^1\Sigma_u^+$
$^3P_0$	$^3P_0$	43 700	$^1\Sigma_g^+(2)$, $^1\Sigma_u^-$, $^1\Pi_g$, $^1\Pi_u$, $^1\Delta_g$, $^3\Sigma_u^+(2)$, $^3\Sigma_g^-$, $^3\Pi_g$, $^3\Pi_u$, $^3\Delta_u$, $^5\Sigma_g^+(2)$, $^5\Sigma_u^-$, $^5\Pi_g$, $^5\Pi_u$, $^5\Delta_g$
$^2S(+)$	$^2P(-)$	?	$^1\Sigma_g^+$, $^1\Sigma_u^+$, $^1\Pi_g$, $^1\Pi_u$, $^3\Sigma_g^+$, $^3\Sigma_u^+$, $^3\Pi_g$, $^3\Pi_u$
^1P	^1P	70 102	$^1\Sigma_g^+(2)$, $^1\Sigma_u^-$, $^1\Pi_g$, $^1\Pi_u$, $^1\Delta_g$

The simple valence molecular orbital analysis applies straightforwardly to only three of the valence states $^3\Pi_g$, $^1\Pi_g$, and $^3\Sigma_u^+$. Some Rydberg character may be present in the $^1\Sigma_u^+$ state. For the other nominally "repulsive" states the effects of configuration mixing and the changes in the character of the molecular orbitals from valence to Rydberg must be considered.

The Mg_2 system is treated in this study as a four-electron valence system. A first step in the analysis of the electronic structure can be patterned after the analysis given by Mulliken[20] of the simpler but analogous H_2 and He_2 systems. As Mulliken has noted, the analysis of homonuclear molecules is usefully begun by considering the asymptotic correlation behavior of the states. The Mg_2 $X\,^1\Sigma_g^+$ ground state, as we have seen in Sec. IV, is like the He_2 ground state, and the molecular orbital Hartree–Fock wavefunction is asymptotically equivalent to a valence bond function constructed from Hartree–Fock atomic wavefunctions. Ignoring the core functions we can write the asymptotic behavior symbolically as

$$4\sigma_g^2\,4\sigma_u^2 \rightarrow 3s_A^2\,3s_B^2\ . \tag{V-1}$$

However, the excited states normally are not represented by a single configuration. The configurations needed to correctly describe the excited states asymptotically are most readily envisioned by adding molecular orbitals to the appropriate ionic configurations. The ground state of He_2, for example, is described by the configuration $1\sigma_g^2\,1\sigma_u^2$. Two positive ion states are obtained by one-electron ionization, the $1\sigma_g^2\,1\sigma_u\ (^2\Sigma_u^+)$ state and the $1\sigma_g\,1\sigma_u^2\,(^2\Sigma_g^+)$ state. Both of these states correlate to $He^+(^2S)+He(^1S)$. The lowest excited atom asymptote is $He(2\,^3S)+He(1\,^1S)$, which correlates with $^3\Sigma_g^+$ and $^3\Sigma_u^+$ molecular states. The two configurations required to allow these molecular states to go asymptotically correctly are obtained by adding the appropriate molecular orbital to the two ion state configurations yielding

$$1\sigma_g^2\,1\sigma_u\,2\sigma_u \pm 1\sigma_g\,1\sigma_u^2\,2\sigma_g\ (^3\Sigma_g^+) \tag{V-2}$$

and

$$1\sigma_g^2\,1\sigma_u\,2\sigma_g \pm 1\sigma_g\,1\sigma_u^2\,2\sigma_u\ (^3\Sigma_u^+)\ . \tag{V-3}$$

For each pair of configurations one linear combination yields the neutral asymptote, while the other yields an ion-pair asymptote $He^+(^2S)+He^-(^2S,\ 1s^2\,2s)$. We will have more to say about the ion-pair asymptotes later.

The valence states of Mg important in this study are only the ^1S ground state and the ^3P and ^1P excited states. The Mg_2 excited-state configurations required for correct asymptotic behavior can be analyzed analogously to He_2. For the $Mg(^3P)+Mg(^1S)$ asymptote we have

$$4\sigma_g^2\,4\sigma_u\,5\sigma_g \pm 4\sigma_u^2\,5\sigma_u\ (^3\Sigma_u^+)\ , \tag{V-4}$$

$$4\sigma_g^2\,4\sigma_u\,5\sigma_u \pm 4\sigma_g\,4\sigma_u^2\,5\sigma_g\ (^3\Sigma_g^+)\ , \tag{V-5}$$

$$4\sigma_g^2\,4\sigma_u\,2\pi_u \pm 4\sigma_g\,4\sigma_u^2\,2\pi_g\ (^3\Pi_g)\ , \tag{V-6}$$

$$4\sigma_g^2\,4\sigma_u\,2\pi_g \pm 4\sigma_g\,4\sigma_u^2\,2\pi_u\ (^3\Pi_u)\ , \tag{V-7}$$

with the analogous singlet configurations for the $Mg(^1P)+Mg(^1S)$ asymptote. Since the $5\sigma_g$, $5\sigma_u$, $2\pi_u$, and $2\pi_g$ molecular orbitals correlate adiabatically with $3p$ atomic orbitals, only the ion configurations that go to $Mg(^1S)+Mg^+(^2S)$ are required for the base configurations, i.e.,

$$4\sigma_g^2\,4\sigma_u\ (^2\Sigma_u^+) \text{ and } 4\sigma_g\,4\sigma_u^2\ (^2\Sigma_g^+). \tag{V-8}$$

Linear combinations that go correctly to the $Mg(^3P)+Mg(^3P)$ asymptote can be constructed as simply.

Once the two configuration "base" wavefunctions have been constructed it is necessary to add other configurations which correlate to higher-lying atomic asymptotes and which effect the state under consideration via configuration interaction. The adiabatic molecular correlations to various atomic asymptotes are shown in Table VI. Ion-pair asymptotes are always added when the electron affinities are positive, and it is now being suggested that scattering resonances (e.g., Mg^-) must also be considered in the list.[5,21] From the analysis given by Mulliken for He_2,[20] we can see that such negative ion states, or ion-pair combinations, necessarily follow from the construction of formally correct asymptotic linear combinations of molecular orbital configurations. Taking negative linear combinations in Eqs. (V-2) and (V-3) yields an ion-pair asymptote $He^+(^2S)+He^-(^2S,\ 1s^2 2s)$. The same thing is true for the negative linear

TABLE VII. Asymptotic forms of the Mg_2 valence molecular orbitals.

Molecular orbital	Atomic combination
$4\sigma_g$	$\frac{1}{\sqrt{2}}\,[3s_A+3s_B]$
$4\sigma_u$	$\frac{1}{\sqrt{2}}\,[3s_A-3s_B]$
$5\sigma_g$	$\frac{1}{\sqrt{2}}\,[3p\sigma_A+3p\sigma_B]$
$5\sigma_u$	$\frac{1}{\sqrt{2}}\,[3p\sigma_A-3p\sigma_B]$
$2\pi_u$	$\frac{1}{\sqrt{2}}\,[3p\pi_A+3p\pi_B]$
$2\pi_g$	$\frac{1}{\sqrt{2}}\,[3p\pi_A-3p\pi_B]$

combinations for Mg_2 in Eqs. (V-4)–(V-7). In fact, all of the bound Rydberg states have their resonance ion-pair complements, and, for a given variational calculation, the computed energy asymptotes (Rydberg vs ion-pair) are determined by the basis set.

It is important to point out that the $He^-(^2S,\ 1s^2\ 2s)$ and $Mg^-(^2P,\ 3s^2\ 3p)$ configurations *do not* represent possible bound ion states. If a variational calculation were performed at large distances on the ion-pair states, the $2s$ (or $3p$) function would yield a zero energy continuum function in the limit of a sufficiently diffuse basis set. These states are more correctly thought of as scattering resonances.[21] For specific kinetic energies the incident electron can be resonantly scattered. This implies that the continuum electron can penetrate a barrier and find an effective potential well attractive enough to change the phase of the function by π. Since the electron can penetrate the valence region, it is possible that such negative ion states could play a role in molecular binding.[21] But as we have seen the ion-pair configurations are already contained in the base wavefunctions and are consequently mixed in the configuration interaction of all these states. The amount of mixing and the significance of ion-pair configurations in these states is best seen by analyzing them singly, since the mixing of all valence, Rydberg, and continuum asymptotes is important and different for each state.

As pointed out in Sec. II, we are also concerned with valence–Rydberg mixing, especially for the high-lying molecular singlet states. Since all Rydberg levels are the result of single electron excitation, their effect on the valence states is included by the SCF optimization of the molecular orbitals rather than by explicit inclusion of singly excited configurations. Unfortunately, extensive optimization of the STF basis set as a function of internuclear distance would have been prohibitively expensive, so we are left with trying to infer Rydberg mixing by looking at the diffuseness of the valence orbitals within the basis set chosen. This may cause an underestimate of the importance of Rydberg character in the wavefunctions.

To insure proper consideration of states arising from the $^3P+^3P$ asymptote it is necessary to include configurations in which two electrons occupy a p-type molecular orbital. This has been done for each of the states under consideration.

MCSCF calculations are usually performed with a relatively small number of configurations. In this study we have considered only excitations within the valence level consisting of molecular orbitals that go asymptotically to either $3s$ or $3p$ atomic orbitals. But, as mentioned above, the molecular orbitals can be quite different in character at shorter internuclear distances, which helps to incorporate many effects. However, because the list of configurations is rather small, there is an inherent difficulty in obtaining the correct relative energies of configurations of different types which are all restricted to be constructed from the same molecular orbitals. For this reason different correlation effects may not be included at the same level of accuracy. This is also true for the asymptotic behavior. The calculated asymptotic states in this study are usually Hartree–Fock-like atoms with at best a small amount of intra-atomic correlation. The ion pair or ionic states have a very different correlation energy behavior than

TABLE VIII. Configuration occupancies for the excited singlet states of Mg_2. Numbers in brackets represent the total number of spin and angular momentum couplings included.

State		Configuration no.	$4\sigma_g$	$4\sigma_u$	$5\sigma_g$	$5\sigma_u$	$2\pi_u$	$2\pi_g$	Couplings
$^1\Sigma_u^+$		1	2	1	1	0	0	0	[1]
		2	1	2	0	1	0	0	[1]
		3	1	1	0	0	2	0	[1]
		4	1	1	0	0	0	2	[1]
		5	1	0	2	1	0	0	[1]
		6	0	1	1	2	0	0	[1]
		7	2	0	0	0	1	1	[1]
		8	0	2	0	0	1	1	[1]
		9	1	0	0	1	2	0	[1]
		10	1	0	0	1	0	2	[1]
		11	0	1	1	0	2	0	[1]
		12	0	1	1	0	0	2	[1]
		13	2	0	1	1	0	0	[1]
		14	0	2	1	1	0	0	[1]
		15	0	0	2	0	1	1	[1]
	[a]	16	0	0	0	2	1	1	[1]
		17	1	1	2	0	0	0	[1]
		18	1	1	0	2	0	0	[1]
$2\,^1\Sigma_g^+$		1	2	2	0	0	0	0	[1]
		2	1	2	1	0	0	0	[1]
		3	2	1	0	1	0	0	[1]
	[a]	4	1	0	1	0	2	0	[1]
		5	0	1	0	1	2	0	[1]
		6	2	0	2	0	0	0	[1]
		7	2	0	0	2	0	0	[1]
		8	2	0	0	0	2	0	[1]
		9	2	0	0	0	0	2	[1]
	[a]	10	0	2	2	0	0	0	[1]
		11	0	2	0	0	2	0	[1]
		12	0	2	0	0	0	2	[1]
		13	1	1	1	1	0	0	[2]
	[a]	14	1	1	0	0	1	1	[2]
		15	1	0	0	1	1	1	[2]
		16	0	1	1	0	1	1	[2]
$^1\Pi_u$		1	1	2	0	0	1	0	[1]
		2	2	1	0	0	0	1	[1]
		3	1	0	2	0	1	0	[1]
		4	1	0	0	2	1	0	[1]
		5	0	1	2	0	0	1	[1]
		6	0	1	0	2	0	1	[1]
		7	1	0	0	0	1	2	[3]
		8	0	1	0	0	2	1	[3]
		9	2	0	1	0	1	0	[1]
		10	0	2	1	0	1	0	[1]
		11	2	0	0	1	0	1	[1]
	[a]	12	0	2	0	1	0	1	[1]
		13	1	0	0	0	3	0	[1]
		14	0	1	0	0	0	3	[1]
$^1\Pi_g$		1	1	2	0	0	0	1	[1]
		2	2	1	0	0	1	0	[1]
		3	1	0	0	2	0	1	[1]
		4	0	1	2	0	1	0	[1]
		5	0	1	0	2	1	0	[1]
		6	1	0	0	0	2	1	[3]
		7	0	1	0	0	1	2	[2]
		8	1	1	1	0	1	0	[2]
		9	1	1	0	1	0	1	[2]
		10	0	1	0	0	3	0	[1]
	[a]	11	1	0	0	0	0	3	[1]
		12	1	0	1	1	1	0	[2]
		13	0	1	1	1	0	1	[2]

[a] Configurations added by configuration interaction (CI).

TABLE IX. Configuration occupancies for the excited triplet states of Mg_2. Numbers in brackets represent the total number of spin and angular momentum couplings included.

State	Configuration no.	$4\sigma_g$	$4\sigma_u$	$5\sigma_g$	$5\sigma_u$	$2\pi_u$	$2\pi_g$	Couplings
$^3\Sigma_u^+$	1	1	2	0	1	0	0	[1]
	2	2	1	1	0	0	0	[1]
	3	1	1	0	0	2	0	[2]
	4	1	1	0	0	0	2	[2]
	5	1	0	2	1	0	0	[1]
	6	0	1	1	2	0	0	[1]
	7	2	0	0	0	1	1	[1]
	8	0	2	1	1	0	0	[1]
	9	2	0	1	1	0	0	[1]
	[a] 10	1	0	0	1	2	0	[1]
	[a] 11	1	0	0	1	0	2	[1]
	12	0	1	1	0	2	0	[1]
	13	0	1	1	0	0	2	[1]
	[a] 14	1	1	2	0	0	0	[1]
	15	1	1	0	2	0	0	[1]
$^3\Sigma_g^+$	1	1	2	1	0	0	0	[1]
	2	2	1	0	1	0	0	[1]
	3	1	0	1	2	0	0	[1]
	4	1	0	1	0	2	0	[1]
	5	1	0	1	0	0	2	[1]
	6	0	1	2	1	0	0	[1]
	7	0	1	0	1	2	0	[1]
	8	0	1	0	1	0	2	[1]
	9	1	1	0	0	1	1	[3]
	10	0	0	1	1	1	1	[3]
$^3\Pi_u$	1	1	2	0	0	1	0	[1]
	2	2	1	0	0	0	1	[1]
	3	1	0	2	0	1	0	[1]
	4	1	0	0	2	1	0	[1]
	5	0	1	2	0	0	1	[1]
	6	0	1	0	2	0	1	[1]
	7	1	0	0	0	1	2	[4]
	8	0	1	0	0	2	1	[4]
$^3\Pi_g$	1	1	2	0	0	0	1	[1]
	2	2	1	0	0	1	0	[1]
	3	1	0	2	0	0	1	[1]
	4[b]	1	0	0	2	0	1	[1]
	5	0	1	2	0	1	0	[1]
	6	0	1	0	2	1	0	[1]
	7	1	0	0	0	2	1	[4]
	8	0	1	0	0	1	2	[4]
	9	1	1	1	0	1	0	[2]
	[a] 10	1	1	0	1	0	1	[2]
	[a] 11	0	1	0	0	3	0	[1]
	[a] 12	1	0	0	0	0	3	[1]
	[a] 13	1	0	1	1	1	0	[2]
	[a] 14	0	1	1	1	0	1	[1]

[a]Configurations added by configuration interaction (CI).
[b]Configurations excluded from the final CI calculation.

TABLE X. Calculated energies[a] for the excited states of Mg_2 arising from the $^1S+^3P$ asymptote.

R(bohr)[b]	$^3\Pi_g$	$^3\Pi_u$	$^3\Sigma_g^+$	$^3\Sigma_u^+$
4.0	−399.15167		−399.02715	−399.10264
4.5	−399.18896	−399.11654		−399.15610
5.0	−399.20438	−399.14422	−399.08651	−399.17949
5.5	−399.20791	−399.15914		−399.18937
6.0	−399.20560	−399.16718	−399.13974	−399.19069
6.5	−399.20038	−399.17156		−399.18798
7.0	−399.19572	−399.17400	−399.16449	−399.18393
7.5	−399.19189	−399.17538		
9.0	−399.18478	−399.17679		−399.17347
12.0	−399.18193	−399.17674		−399.17003
15.0			−399.17404	

[a]Energies in hartree; 1 hartree = 27.212 eV = 219 475 cm^{-1}.
[b]1 bohr = 0.5291772×10^{-8} cm.

TABLE XI. Calculated energies[a] for the excited states of Mg_2 arising from the $^1S+^1P$ asymptote.

R(bohr)[b]	$^1\Pi_g$	$^1\Pi_u$	$2\,^1\Sigma_g^+$	$^1\Sigma_u^+$
4.0	−399.10483	−399.00497	−398.94769	−399.04541
5.0	−399.15164	−399.07555	−399.04739	−399.11382
5.5	−399.15199	−399.08471	−399.07587	−399.12246
6.0	−399.14657	−399.08624	−399.09328	−399.12445
7.0	−399.13031	−399.08064	−399.10483	−399.12060
8.0	−399.11518	−399.07589	−399.10027	−399.11423
15.0	−399.08597	−399.08319	−399.08737	−399.09395
∞[c]	−399.08388	−399.08528	−399.09154	−399.08978

[a]Energies in hartree; 1 hartree = 27.212 eV = 219 475 cm^{-1}.
[b]1 bohr = 0.5291772×10^{-8} cm.
[c]Asymptotic energies calculated by adding dipole–dipole resonance interactions to the R = 15 bohr values using $\mu_z^2 = 7.03$ a.u.

the low-lying valence states, and the Hartree–Fock asymptotic energy differences are likely to be considerably in error. When the valence states are being optimized, the higher-lying roots are necessarily too high. For ion-pair states this may seriously distort the mixing at small distances.

The configuration lists used in the calculations are tabulated for each state in Tables VIII and IX. The asymptotic forms of the molecular orbitals are given in Table VII. In some cases, in order to save time, a half dozen to a dozen of the dominant configurations for a given state were used in a full MCSCF calculation in order to optimize the valence orbitals at each value of R. Then, the remaining configurations were added by a simple configuration interaction procedure with no further orbital optimization. The total number of configurations (including all spin and angular momentum couplings) was restricted to 20 in each case, so some of the least important configurations (or couplings) were excluded from the lists. In the case of the $2\,^1\Sigma_g^+$ state the configurations were constructed from molecular orbitals that were optimized in the $^1\Sigma_u^+$ calculation. For that reason we expect the $2\,^1\Sigma_g^+$ results to be the least accurate, but we still feel that the principal features of the state are well represented.

B. Results and analysis for individual states

The calculated potential energy curves for the eight excited valence states of Mg_2 are tabulated in Tables X and XI and plotted in Fig. 4. In the plot the calculated asymptotic energy for each state was set equal to the known separated atom asymptote. For the triplet states arising from $^3P+^1S$ the calculated energy at R = 12 bohr was taken to be the asymptotic energy. For the singlet states arising from $^1P+^1S$ the dipole–dipole resonance interactions[22] proportional to $\mu_z^2 R^{-3}$ were added to the R = 15 bohr energies to obtain the asymptotic limits. A calculated atomic value of $\mu_z^2 = 7.03$ a.u. from our R = 15 bohr wavefunctions was used. Since the states differ considerably in character, it is best to analyze each individually.

1. The $^1\Sigma_u^+$ state

The $^1\Sigma_u^+$ state of Mg_2 is the only excited state that has been accurately characterized spectroscopically. The

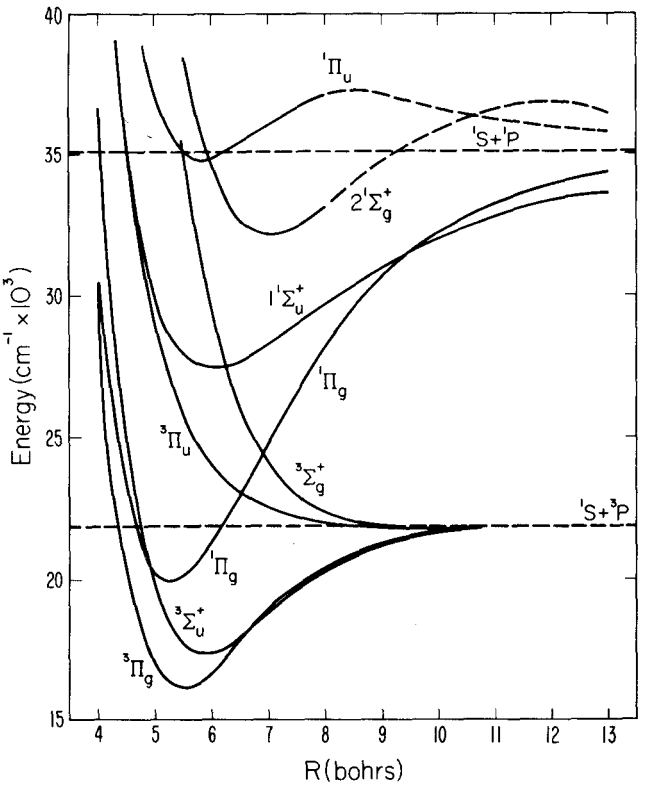

FIG. 4. Potential energy curves for the excited valence states of Mg_2. The dashed portions of the $^1\Pi_u$ and $2\,^1\Sigma_g^+$ curves indicate regions that have not been investigated directly, but are estimated by joining known short-range and long-range behavior.

first published spectrum that we could find was taken by Hamada[1] in 1931. He observed a strong continuum with a maximum at 388 nm, which he ascribed to bound Mg_2 molecules correlating with the Mg $2\,^1P_1$ atomic state. Later observations include those of Strukov[23] and Weniger,[24] who both reported banded spectra to the red and to the blue of the Mg 258.2 nm $1\,^1S_0 - 2\,^1P_1$ resonance line. The first highly resolved spectra of Mg_2 were taken by Balfour and Douglas in 1969.[2] Recently, Vidal and Scheingraber[25] have reanalyzed the absorption spectra of Balfour and Douglas[2] and have produced an RKR curve for the $^1\Sigma_u^+$ state as shown in Fig. 5.

Asymptotically, the $^1\Sigma_u^+$ state is described by the configurations $4\sigma_g^2\,4\sigma_u\,5\sigma_g$ and $4\sigma_g 4\sigma_u^2\,5\sigma_u$. Near R_e the first configuration becomes dominant with no indication of a curve crossing at any R value. The long range part of the potential is dominated by $-2\mu_z^2 R^{-3}$, and our calculated value of μ_z^2 is 7.3 a.u. at $R = 15$ bohr. This value is about 25% larger than the experimental value of 5.67 a.u.[26] In our calculation we added all important valence single and double excitations to the two base configurations. An important part of the R dependence of the electronic correlation energy is not included since we omitted doubly excited configurations in which one electron is excited within the valence level and the other electron is excited to a virtual orbital. Since such configurations contribute more correlation energy as the atom–atom overlap increases, we expect our calculated potential energy curve to be less bound than the experimental one. Some of our computed energy points are plotted in Fig. 5 for comparison with the RKR curve. Our R_e value is close to the experimental one, but the D_e is too small by about 1800 cm^{-1} relative to the experimental D_e of 9387 cm^{-1} as anticipated. This comparison provides a good basis for estimating the accuracy of the calculated potential energy curves for the other states.

The only nonvalence behavior to be noticed in the $^1\Sigma_u^+$ state is the mixing of considerable diffuse 4s character into the $5\sigma_g$ orbital at small values of R as shown in Table XII. This may be an indication of valence-Rydberg mixing of the $Mg_2^+\,^2\Sigma_u^+$ ion.

2. The $^1\Pi_u$ state

The asymptotic configurations for the $^1\Pi_u$ state are $4\sigma_g\,4\sigma_u^2\,2\pi_u$ and $4\sigma_g^2\,4\sigma_u\,2\pi_g$. The long-range interaction is $+\mu_z^2 R^{-3}$. These two facts would prompt one to predict that the $^1\Pi_u$ state is unbound. However, spectroscopic evidence has been presented which infers a bound or quasibound level close to and above the $^1\Sigma_u^+$ state.[2,23]

Our MCSCF calculations revealed a bound $^1\Pi_u$ state with a large barrier (~2000 cm^{-1}) at about 8 bohr. The results are very similar to the results of Hay *et al.*[5] for Zn_2. The $^1\Pi_u$ mixing coefficients in Table XIII and the potential energy curves for the two lowest $^1\Pi_u$ states in Fig. 6 show a definite curve crossing phenomenon. Between 8 and 7.5 bohr the wavefunction changes very abruptly from two dominant configurations to one. The unusual distortions of the $2\,^1\Pi_u$ curve in Fig. 6 are prob-

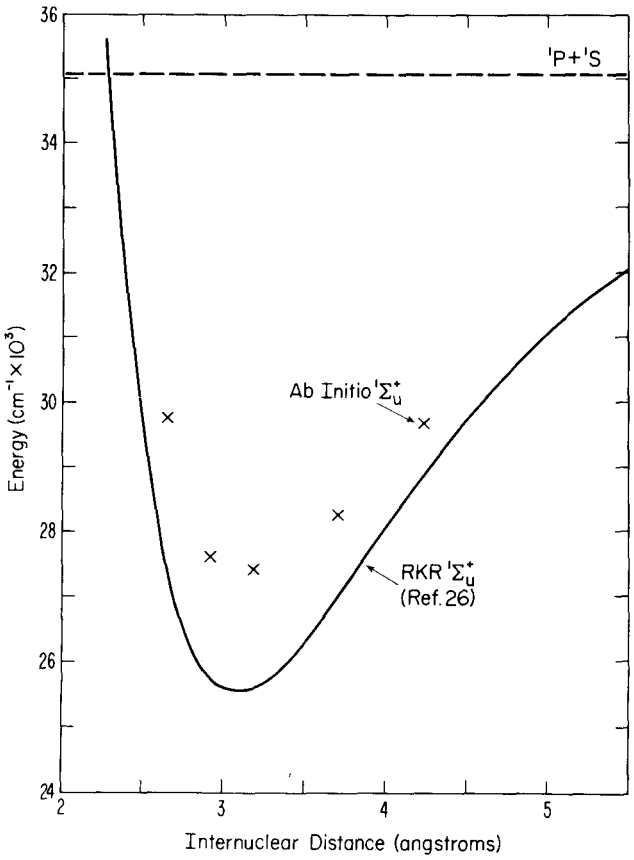

FIG. 5. Comparison of theoretical and experimental (RKR) potential energy curves for the $^1\Sigma_u^+$ state of Mg_2.

TABLE XII. Expansion coefficients for the principal $^1\Sigma_u^+$ molecular orbitals at long range and near R_e.

STF (exponent)	$4\sigma_g$		$4\sigma_u$		$5\sigma_g$	
	$R=15$ bohr	$R=6$ bohr	$R=15$ bohr	$R=6$ bohr	$R=15$ bohr	$R=6$ bohr
1s(14.161)	0.02702	0.02485	0.02746	0.02855	0.00004	0.00432
2s(12.228)	0.01719	0.01571	0.01748	0.01829	0.00001	0.00251
3s(7.091)	−0.02255	−0.01770	−0.02251	−0.02525	0.00053	0.00318
2s(3.499)	−0.15262	−0.15281	−0.15606	−0.15357	−0.00192	−0.05268
3s(1.458)	0.37184	0.32617	0.38320	0.41606	−0.00457	0.02509
3s(0.891)	0.39757	0.30347	0.39151	0.46720	−0.00041	−0.06756
2p(8.527)	0.00034	−0.00159	0.00002	0.00188	−0.00442	−0.00806
2p(4.705)	0.00180	−0.00382	0.00186	0.01235	−0.03346	−0.04216
2p(2.719)	0.00234	−0.01190	0.00018	0.01501	−0.03038	−0.05774
3p(1.168)	−0.01079	0.05100	−0.00176	−0.06740	0.14495	0.25553
3p(0.560)	−0.02305	−0.03478	−0.03100	0.02637	0.54547	0.42902
3d(2.000)	−0.00273	0.00448	−0.00249	−0.00985	−0.00178	0.00886
3d(0.600)	−0.02238	0.02105	−0.03915	−0.05071	0.01857	0.09506
4s(0.600)	−0.00931	0.04376	−0.03071	−0.01557	0.00813	−0.31484

ably due to the fact that the molecular orbitals are optimized for the lowest state and hence do not provide a good representation of the charge transfer state in the curve crossing region. The $1/R$ curve in the figure clearly shows the charge transfer nature of the crossing.

The principal $^1\Pi_u$ molecular orbitals tabulated in Table XIV do not show much deviation from valence character as a function of R. The $2\pi_g$ orbital becomes more diffuse at $R=6$ bohr, which may indicate mixing with the $4p$ Rydberg of the $^2\Sigma_u^+$ ion or the characteristics of the ion pair state. Unfortunately, we did not anticipate this mixing and the basis set does not contain STF's appropriate for a description of p-type Rydberg character.

It is easy to see why the $^1\Pi_u$ state should exhibit a charge transfer curve crossing while the $^1\Sigma$ states do not. First, the $4p$ Rydberg states lie considerably higher in energy (6000–7000 cm^{-1}) than the 4s Rydbergs, and they are crossed by the $1/R$ charge transfer state at much larger values of R. For this reason the Rydberg mixing with the valence and charge transfer states is much less for the Π states in the region near 6 bohr. Secondly, and more important, the $^1\Pi_u$ configuration arising from the $^3P+^3P$ asymptote ($4\sigma_g^2 5\sigma_g 1\pi_u$) is not as strongly bound as the $^1\Sigma_g^+$ configuration ($4\sigma_g^2 5\sigma_g^2$), and consequently does not lie below the $1/R$ charge transfer potential in the molecular region. In our $^1\Pi_u$ calculation the effect of the $4\sigma_g^2 5\sigma_g 1\pi_u$ configuration is probably underestimated because the $5\sigma_g$ orbital was not optimized with that configuration in the MCSCF configuration list.

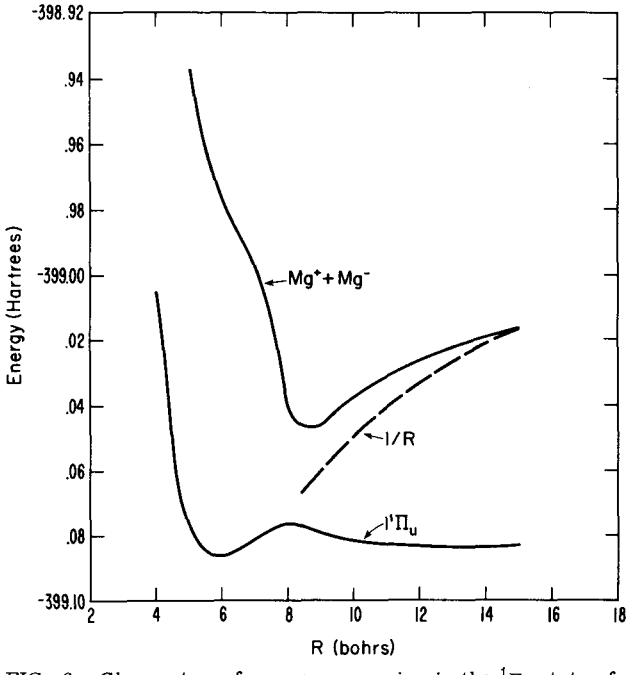

FIG. 6. Charge transfer curve crossing in the $^1\Pi_u$ state of Mg_2 (1 hartree = 219474.6 cm^{-1}; 1 bohr = 0.5291772×10^{-8} cm).

The long-range potentials of the Σ and Π ion-pair states are also split by anisotropic ionic interactions such as the ion–quadrupole. Although these differences are small compared to the R^{-1} Coulombic term, they still may be significant in determining the relative importance of the ion-pair configuration at a given internuclear separation. The Π states would be lower in energy than the Σ states. However, we are not able to

TABLE XIII. Configuration mixing coefficients for the Mg_2 $^1\Pi_u$ state.

Configuration no.	$R=7$ bohr	$R=7.5$ bohr	$R=8$ bohr	$R=15$ bohr
1	−0.03768	0.02826	0.53359	0.72731
2	0.97639	0.97625	0.83309	0.66973
3	0.01955	0.01677	−0.00129	−0.00033
4	0.00373	0.00144	−0.03473	−0.04759
5	−0.11456	−0.11347	−0.00256	−0.00036
6	−0.03873	−0.03904	−0.04198	−0.03849
7	−0.05361	−0.06070	−0.07850	−0.08708
8	−0.06238	−0.06879	−0.03853	−0.03569
9	−0.07153	−0.07022	−0.04416	−0.02661
10	−0.13499	−0.13445	−0.08676	−0.08203
11	−0.00593	−0.00266	0.02183	0.03970
12	0.00932	0.00491	−0.02572	−0.02950

TABLE XIV. Expansion coefficients for the principal $^1\Pi_u$ state molecular orbitals at long range and near R_e.

STF	$4\sigma_g$		$4\sigma_u$		$2\pi_g$	
(exponent)	$R = 15$ bohr	$R = 6$ bohr	$R = 15$ bohr	$R = 6$ bohr	$R = 15$ bohr	$R = 6$ bohr
1s(14.161)	−0.02745	−0.02504	−0.02738	−0.02856		
2s(12.228)	−0.01747	−0.01579	−0.01743	−0.01843		
3s(7.091)	0.02253	0.01675	0.02263	0.02747		
2s(3.499)	0.15576	0.15894	0.15532	0.14143		
3s(1.458)	−0.38289	−0.32385	−0.38051	−0.43576		
3s(0.891)	−0.39269	−0.28123	−0.39595	−0.53511		
2p(8.527)	0.00007	0.00331	0.00003	−0.00280	−0.00494	−0.00234
2p(4.705)	−0.00005	0.01335	0.00007	−0.01362	−0.03738	−0.03987
2p(2.719)	0.00051	0.02444	0.00019	−0.02185	−0.03393	−0.01522
3p(1.168)	−0.00218	−0.10678	−0.00109	0.08874	0.16986	0.08856
3p(0.560)	0.00096	−0.04680	−0.00115	−0.07172	0.60866	0.97559
3d(2.000)	−0.00149	−0.00668	−0.00138	0.00478	0.00000	−0.00336
3d(1.000)	−0.01734	−0.03965	−0.01722	−0.03412	−0.00716	−0.04763
4s(1.000)	0.02373	0.01474	0.02072	−0.05160		

separate out the diagonal and off diagonal effects that yield a given result and conclude that our data can only be interpreted as an ion-pair dominant state if the Coulombic interaction is obvious. Note from Fig. 6 that the asymptotic ion-pair energy is near −398.97 hartree, which is close to the calculated $Mg^+(^2S) + Mg(^1S)$ asymptote.

The $^1\Pi_u$ state is the only Mg_2 valence excited state for which we could find conclusive evidence of a curve crossing with the resonance scattering state $Mg^+ Mg^-$.

3. The $^1\Pi_g$ state

The $^1\Pi_g$ state of Mg_2 is the easiest of the singlet states to understand. Asymptotically, it is described by the configurations $4\sigma_g^2\ 4\sigma_u\ 2\pi_u$ and $4\sigma_g\ 4\sigma_u^2\ 2\pi_g$. But, as the molecule forms, the first configuration becomes dominant. The bonding characteristics of this configuration are augmented by the long-range dipole–dipole resonance attraction given by $-\mu_z^2 R^{-3}$. The molecular orbitals near R_e remain dominantly valencelike with a slight contraction of the $4\sigma_g$ and $2\pi_u$ bonding orbitals which increases their bonding character, and a small amount of $3p\sigma$ character mixing into the $4\sigma_u$ orbital (which tends to make it less antibonding due to reduced atom–atom overlap). Ion-pair configuration mixing is present in the sense noted earlier that a single dominant valence configuration is only one of two configurations required to go asymptotically to neutral atoms. But there is no evidence in the potential energy curves or the character of the orbitals of ion-pair mixing. The very attractive $^1\Pi_g$ curve can be attributed to the smaller singlet–triplet exchange splitting in the II states as compared to the asymptotic exchange splitting.

4. The $^3\Pi_g$ state

The $^3\Pi_g$ state is described by the same two configurations asymptotically as the $^1\Pi_g$ state, except for the spin coupling. The $4\sigma_g^2\ 4\sigma_u\ 2\pi_u$ configuration is dominant near R_e, and the orbitals are primarily valencelike as in the case of $^1\Pi_g$. The $^3\Pi_g$ and $^1\Pi_g$ states are split by about 0.5 eV near R_e, which is about what one would expect for the exchange splitting between triplet and singlet II states described by essentially the same configuration.

The $^3\Pi_g$ state is probably the most important metal vapor dimer state from a laser applications point of view. It constitutes the lowest-lying excimer state in the system and is metastable with respect to transitions to the ground state. We expect all homonuclear metal dimer systems to have similar metastable molecular reservoirs. This could impede laser energy extraction on a short time scale (subnanosecond), but should not hinder longer time extraction processes since the splitting between the $^3\Pi_g$ and the $^3\Sigma_u^+$ state is only about 2000 cm^{-1} and the two states can equilibrate fairly rapidly by an exchange process under collision with another Mg atom.

5. The $^3\Sigma_u^+$ state

The $^3\Sigma_u^+$ state constitutes the lowest-lying bound excimer state which can radiate to the ground state by an electric dipole transition. The spin selection rule is broken by spin–orbit mixing of $^3\Sigma_u^+$ with $^1\Pi_u$. This state is likely to be the major source of the first continuum to the red of the $^3P_1 - {}^1S_0$ atomic line in pure homonuclear metal vapor systems.

The $^3\Sigma_u^+$ state is described asymptotically by the configurations $4\sigma_g^2\ 4\sigma_u\ 5\sigma_g$ and $4\sigma_g\ 4\sigma_u^2\ 5\sigma_u$. The first configuration is dominant near R_e and the molecular orbitals remain valencelike in that region.

6. The $^3\Pi_u$ state

The $^3\Pi_u$ state is described throughout the molecular region and asymptotically by the configurations $4\sigma_g^2\ 4\sigma_u\ 2\pi_g$ and $4\sigma_g\ 4\sigma_u^2\ 2\pi_u$. At no point is there a sudden change to single configuration character as in the case of $^1\Pi_u$. Figure 7 shows that the $Mg^+ Mg^-$ charge transfer state lies too far above the lowest $^3\Pi_u$ level for a curve crossing to occur. Consequently, the $^3\Pi_u$ state is unbound as would be predicted by simple covalent molecular orbital theory.

TABLE XV. Configuration mixing coefficients for the $2\,^1\Sigma_g^+$ state of Mg_2.

Configuration no.	$R=5.0$ bohr	$R=7.0$ bohr	$R=15.0$ bohr
1	0.11827	0.16603	0.15508
2	0.43740	0.46036	0.75956
3	−0.29897	−0.32100	0.58882
4	−0.14055	−0.08985	−0.08490
5	0.04681	0.06416	−0.06157
6	0.73504	0.59466	0.01861
7	−0.08418	−0.14156	−0.05639
8	−0.24224	−0.13541	0.03235
9	−0.00429	−0.03038	0.03276
10	−0.22301	−0.39158	−0.06934
11	0.07424	0.08825	0.03899
12	−0.01821	−0.01526	0.03516
13	−0.02435	−0.00198	0.05086
14	−0.10609	−0.28916	0.09139
15	0.06735	0.04292	−0.06926
16	0.04621	0.02895	−0.00946
17	−0.02200	−0.03488	0.06593
18	−0.00840	−0.00267	0.00024
19	0.03933	0.04628	0.08875
20	−0.03314	−0.03648	−0.00733

7. The $2\,^1\Sigma_g^+$ state

The $2\,^1\Sigma_g^+$ state of Mg_2 is obtained by a Brillouin-type single excitation from the $1\,^1\Sigma_g^+$ ground state, and is therefore not compatible with the SCF portion of our MCSCF computer code. For that reason the state was studied in the CI approximation using orbitals which were optimized for the $^1\Sigma_u^+$ state. We still believe, however, that the fundamental characteristics of the state are well represented.

Asymptotically, the $^1\Sigma_g^+$ state requires two configurations $4\sigma_g\,4\sigma_u^2\,5\sigma_g$ and $4\sigma_g^2\,4\sigma_u\,5\sigma_u$ (configurations 2 and 3 in Table VIII). Ordinarily, a state described by such configurations is not expected to be strongly bound. However, it is clear from Fig. 4 that a significant amount of binding does occur. To understand the binding one need only consider that the $^3P+{}^3P$ asymptote, which is just a volt above the $^1P+{}^1S$ asymptote, can give rise to two $^1\Sigma_g^+$ configurations which exhibit substantial binding. These configurations are $4\sigma_g^2\,5\sigma_g^2$ and $4\sigma_g^2\,2\pi_u^2$ (configurations 6 and 8 in Table VIII). The first configuration has two electrons in a bonding orbital formed from two atomic $3p\sigma$ orbitals. Bonds of this type are known to be very strong and can give rise to several volts of binding such as in the case of $N_2(^1\Sigma_g = {}^2D+{}^2D)$.[27] The second configuration, although weaker, can still result in substantial binding relative to the $^3P+{}^3P$ asymptote. We expected these two configurations to mix strongly in the $2\,^1\Sigma_g^+$ state even at large values of R, since the strong bonding effects should overcome the 1 eV excitation energy deficit rather quickly as the molecule is formed. Table XV, which gives the $2\,^1\Sigma_g^+$ configuration mixing coefficients as a function of R, bears out our expectations.

In their discussion of Zn_2 Hay *et al.*[5] indicated that the $2\,^1\Sigma_g^+$ state is dominated by charge transfer through the Zn^+ and Zn^- scattering resonance. In our calculation one could consider that the change in phase of configurations 2 and 3 during molecular formation is an indication of charge transfer. This is not a reliable analysis however, since by the same logic the ground state of $H_2(1\sigma_g^2)$ would have 50% ionic character at R_e. It is much more valid to consider whether the potential energy curve has $1/R$ behavior at large values of R, or if a curve crossing with a higher-lying state that is dominated by $1/R$ is evident. Certainly, our $2\,^1\Sigma_g^+$ curve does not have $1/R$ behavior at any point. The $3\,^1\Sigma_g^+$ state, which is not tabulated, is also bound and widely split (1 eV) from the $2\,^1\Sigma_g^+$ curve at the closest point of approach. A sizeable barrier exists in the $2\,^1\Sigma_g^+$ curve due to the long-range dipole–dipole resonance forces proportional to $2\mu^2 R^{-3}$. The size of this interaction is 0.114 eV at $R=15$ bohr. The only root of our CI Hamiltonian matrix that exhibits $1/R$ behavior is the $6\,^1\Sigma_g^+$. This state becomes repulsive at $R=8$ bohr due to interactions with the lower $4\,^1\Sigma_g^+$ and $5\,^1\Sigma_g^+$ states, which are both repulsive asymptotically. It is possible that this ion-pair state correlates to the $Mg^+(^2P)+Mg^-(^2P)$ asymptote.

The above analysis must be tempered by the fact that the orbitals of the higher-lying $^1\Sigma_g^+$ states have not been properly optimized by the MCSCF procedure, and consequently the charge transfer state is not well represented. Indeed, the $2\,^1\Sigma_g^+$ state in Zn_2, as reported by Hay *et al.*,[5] shows a minimum at much smaller R than the corresponding minimum in Mg_2.

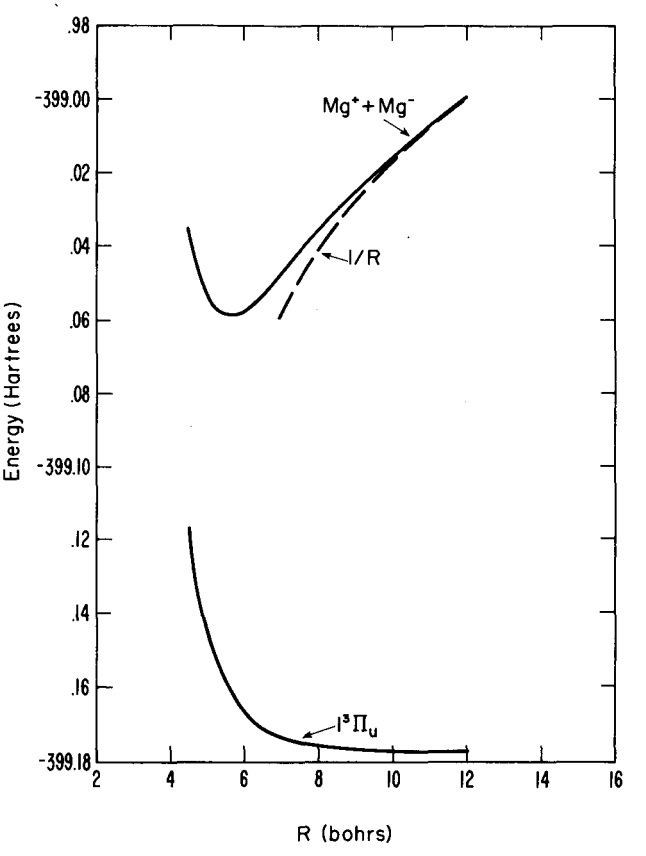

FIG. 7. Valence and charge transfer $^3\Pi_u$ states in Mg_2.

8. The $^3\Sigma_g^+$ state

The $^3\Sigma_g^+$ state reinforces our interpretation of the binding in the $2\,^1\Sigma_g^+$ state. The two states are described asymptotically by the same two configurations $4\sigma_g\ 4\sigma_u^2\ 5\sigma_g$ and $4\sigma_g^2\ 4\sigma_u\ 5\sigma_u$ with different spin couplings. However, there are *no* $^3\Sigma_g^+$ configurations coming out of the $^3P + {}^3P$ asymptote. Consequently, there are no strongly bound configurations that can mix with the $^3\Sigma_g^+$ state, and it is repulsive as anticipated.

The two asymptotic configurations remain dominant from 15 to about 5 bohr. The second root of the CI matrix is the charge transfer state $Mg^+\ Mg^-$, but there is no evidence of a curve crossing at any value of R. For $R < 5$ bohr the $^3\Sigma_g^+$ state becomes a 4s Rydberg of the $Mg_2^+\ ^2\Sigma_u^+$ ion, with the $4\sigma_g^2\ 4\sigma_u\ 5\sigma_u$ configuration being dominant. The $5\sigma_u$ orbital becomes a linear combination of the diffuse 4s STF's.

VI. CONCLUDING REMARKS

The low-lying valence states of Mg_2 have been studied by a combination of multiconfiguration self-consistent-field and configuration interaction techniques with the hope of providing a model for other homonuclear divalent metal dimer systems. The ground state has been found to be essentially repulsive with a small van der Waals well. Theoretical calculation of the ground state potential at intermediate distances is complicated by an apparent strong coupling between inter- and intra-atomic electron correlation components.

Two bound states arise from the $^3P + {}^1S$ asymptote. The lowest-lying excimer state is $^3\Pi_g$, which provides a metastable molecular reservoir that could play an important role in laser and amplifier applications. The bound $^3\Sigma_u^+$ state, which gains dipole transition strength to the ground state via spin–orbit coupling with the $^1\Pi_u$ state, is believed to be the dominant source of continuum radiation to the red of the ^3P–^1S atomic transition in all homonuclear metal vapor dimer systems. All of the triplet molecular states are qualitatively described by simple covalent molecular orbital theory.

All of the states arising from the $^1P + {}^1S$ asymptote are found to be bound, and all for different reasons. The $2\,^1\Sigma_g^+$ state exhibits strong mixing with the bound $4\sigma_g^2\ 5\sigma_g^2$ configuration coming out of the $^3P + {}^3P$ asymptote. The $^1\Pi_u$ state, although repulsive asymptotically, undergoes a curve crossing with a charge transfer state associated with the Mg^+Mg^- scattering resonance. This gives rise to a large barrier in the potential at $R = 8$ bohr. The $^1\Sigma_u^+$ and $^1\Pi_g$ states are predominantly valence-like, although the $^1\Sigma_u^+$ state does show signs of Rydberg character near R_e. The only state which we can unambiguously characterize as charge transfer dominated is the $^1\Pi_u$ state. Even in that case, however, our basis set was not sufficiently flexible to describe p-type Rydberg states of the $Mg_2^+\ ^2\Sigma_u^+$ molecular ion.

ACKNOWLEDGMENTS

The authors would like to thank Drs. P. J. Hay, T. Dunning, H. Scheingraber, and C. R. Vidal for making copies of their manuscripts available prior to publication.

[1]H. Hamada, Philos. Mag. **12**, 50 (1931).
[2]W. J. Balfour and A. E. Douglas, Can. J. Phys. **48**, 901 (1970).
[3]H. Scheingraber, Thesis, Max Planck Institüt für Physik und Astrophysik (1975).
[4]C. F. Bender and E. R. Davidson, J. Chem. Phys. **47**, 4972 (1967).
[5]P. J. Hay, T. H. Dunning, and R C. Raffenetti, J. Chem. Phys. **65**, 2679 (1976).
[6]H. Scheingraber and C. R. Vidal, Proceedings of the 3rd Summer Colloquium on Electronic Transition Lasers (1976).
[7]G. Das and A. C. Wahl, "BISON-MC: A FORTRAN Computing System for Multiconfiguration Self-Consistent-Field Calculations on Atoms, Diatoms, and Polyatoms," Argonne National Laboratory Report No. ANL 7955 (1972).
[8]P. S. Bagus, T. L. Gilbert, and C. C. J. Roothaan, J. Chem. Phys. **56**, 5195 (1972).
[9]E. Clementi and C. Roetti, At. Data **14**, 177 (1974).
[10]E. A. Reinsch and W. Meyer, Phys. Rev. A **14**, 915 (1976).
[11]F. H. Mies, Mol. Phys. **26**, 1233 (1973).
[12]W. C. Stwalley, Chem. Phys. Lett. **7**, 600 (1970); J. Chem. Phys. **54**, 4517 (1971); K. C. Li and W. C. Stwalley, J. Chem. Phys. **59**, 4423 (1973).
[13]P. J. Bertoncini and A. C. Wahl, Phys. Rev. Lett. **25**, 991 (1970); G. Das and A. C. Wahl, Phys. Rev. A **4**, 825 (1971).
[14]P. J. Bertoncini and A. C. Wahl, J. Chem. Phys. **58**, 1259 (1973).
[15]B. Liu and D. McLean, J. Chem. Phys. **59**, 4557 (1973).
[16]G. Das and A. C. Wahl, Phys. Rev. A **4**, 825 (1971).
[17]A. F. Wagner, G. Das, and A. C. Wahl, J. Chem. Phys. **60**, 1885 (1974).
[18]W. J. Stevens, A. C. Wahl, M. A. Gardner, and A. Karo, J. Chem. Phys. **60**, 2195 (1974).
[19]J. P. Desclaux, At. Data Nucl. Data Tables **12**, 312 (1973).
[20]R. S. Mulliken, J. Am. Chem. Soc. **88**, 1849 (1966).
[21]H. S. Taylor, F. W. Bobrowicz, P. J. Hay, and T. H. Dunning, J. Chem. Phys. **65**, 1182 (1976).
[22]G. W. King and J. H. Van Vleck, Phys. Rev. **55**, 1165 (1939).
[23]V. S. Strukov, Opt. Spectrosc. (USSR) **14**, 184 (1963).
[24]P. S. Weniger, J. Phys. (Paris) **25**, 946 (1964).
[25]C. R. Vidal and H. Scheingraber, J. Mol. Spectrosc. (to be published).
[26]A. W. Weiss, J. Chem. Phys. **47**, 3573 (1967).
[27]H. H. Michels, J. Chem. Phys. **53**, 841 (1970).